gated above that nonconical rotational flows of the given classes — double shocks — exist only in the exceptional case of an adiabatic exponent $\gamma = 2$. The constructed solution (3.9) shows that this situation does not occur in unsteady three-dimensional flow, while nonconical rotational triple shocks with rectilinear level lines exist for any values of γ.

LITERATURE CITED

1. L. V. Ovsyannikov, "A new solution of the hydrodynamical equations," Dokl. Akad. Nauk SSSR, 111, No. 1 (1956).
2. O. I. Bogoyavlenskii and S. P. Novikov, "Homogeneous models in general relativity theory and gasdynamics," Usp. Mat. Nauk, 31, No. 5(191) (1976).
3. L. Rosenhead, Laminar Boundary Layers, Clarendon Press, Oxford (1963).
4. L. D. Landau and E. M. Lifshits, Continuum Mechanics [in Russian], GITTL, Moscow (1954).
5. A. F. Sidorov, "Unsteady potential motions of a polytropic gas with a degenerate hodograph," Prikl. Mat. Mekh., 23, No. 5 (1959).
6. A. F. Sidorov, "Exact triple-shock solutions of the gasdynamical equations," Dokl. Akad. Nauk SSSR, 194, No. 4 (1970).
7. A. F. Sidorov and N. N. Yanenko, "Unsteady planar flows of a polytropic gas with rectilinear characteristics," Dokl. Akad. Nauk SSSR, 123, No. 5 (1958).
8. E. N. Zubor, "Steady three-dimensional flows of an ideal gas with a degenerate hodograph when the Bernoulli integral holds," in: Proc. Inst. Math. Mech., Ural Sci. Center, Acad. Sci. USSR, Methods of Solution of Boundary-Value Problems in Continuum Mechanics [in Russian], No. 25 (1978).

MODELS AND SIMILARITY ANALYSIS IN THE THERMODYNAMICS OF

GAS—LIQUID SYSTEMS

S. S. Kutateladze

UDC 536.24

Fundamental similarity numbers are considered for heat transfer and dynamics in gas-liquid systems, including effects due to change of state and loss of stability.

Introduction. Mikhail Alekseevich Lavrent'ev is a great master who has produced clear and efficient physicomathematical models in hydrodynamics.

There are numerous relevant factors in the thermohydrodynamics of multiphase systems, and the flows have a multiplicity of structure, so such models are particularly important. Therefore, we hope that a compact exposition of some results in this area will constitute a tribute.

Some of the complicated problems in thermokinetics and mechanics of flowing media arise in the dynamics of gas—liquid systems, particularly in energy transport in phase transitions.

The following features are the most important:

1. The variety of dynamic structures and the variability in the spontaneous formations (bubbles, droplets, films, and jets) in space and time.

2. The wave effects at interfaces and within mixtures related to surface tension and the substantial dependence of signal transmission speeds on component concentrations and element structures.

3. Effects from the thermohydrodynamics of primary nucleation and the distribution of condensation centers at boundaries and within the flow.

4. The scope for states essentially metastable in the thermodynamic sense.

5. The complications of turbulent transport related to features of the flow in the elements of each phase, in addition to the common interphase turbulence.

6. Quasiturbulent states can occur in a laminar flow on account of oscillations of dispersed elements of the other phase.
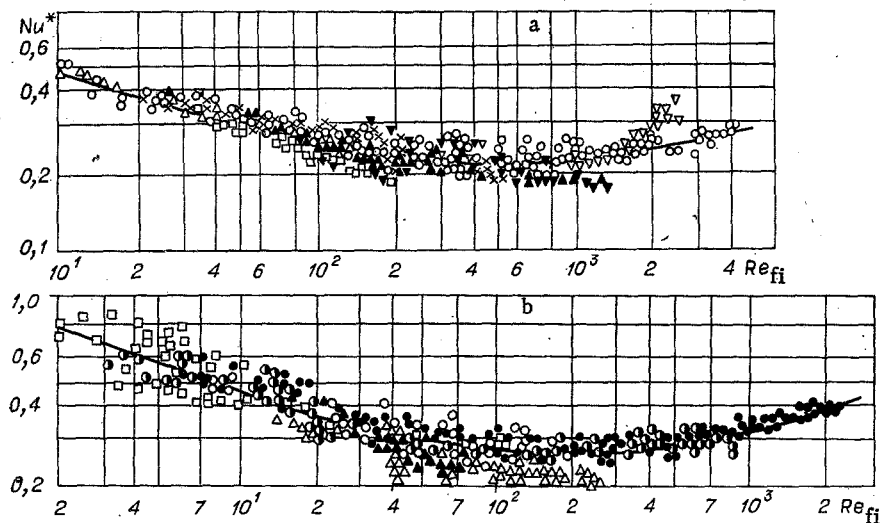
Fig. 1

Internal Linear Scales in the Presence of a Phase Interface. A large part is played in the theory of single-phase boundary layers by the internal dynamic linear dimensions, which are constructed from the momentum and energy flux desnity (the momentum-loss thickness, the energy-loss thickness, and the displacement thickness). One gets internal characteristic dimensions in a system with phase interfaces that are related to interaction with external fields and to surface effects.

The difference in density of the phases means that there are local Archimedean forces, which interact with the viscous forces, surface tension, dynamic pressure, etc.

For example, the gravitational-viscous interaction in a freely flowing film of viscous liquid may be assigned the linear scale

$$\delta_v = \left[\frac{v'^2}{g \left(1 - \frac{\rho''}{\rho'} \right)} \right]^{1/3}.$$

Another important characteristic of this kind is the linear scale for the capillary-gravitational interaction:

$$\delta_\sigma = \left[\frac{\sigma}{g \left(\rho' - \rho'' \right)} \right]^{1/2}.$$

This corresponds to the scale of the propagation speed for the capillary-gravitational waves:

$$u_\sigma = \left(\frac{g\sigma}{\rho' - \rho''} \right)^{1/4}.$$

A kinematic characteristic for the mass transfer in phase transition can be formed from the flux density for the new phase. For example, the average rate of vapor production can be written as

$$U'' = \frac{q}{r\rho''},$$

while the momentum transferred to the liquid by the vapor generated at the heating surface is put as

$$j_w'' = \frac{q}{r}.$$

When a liquid bubbles through a gas via a microporous surface, U" is the volume bubbling rate:

$$j_w'' = \rho'' U''.$$

The linear scale characterizing the scope for occurrence of a new phase is the minimum nucleation radius allowing of thermodynamic equilibrium. For example, for the nucleus of a vapor bubble
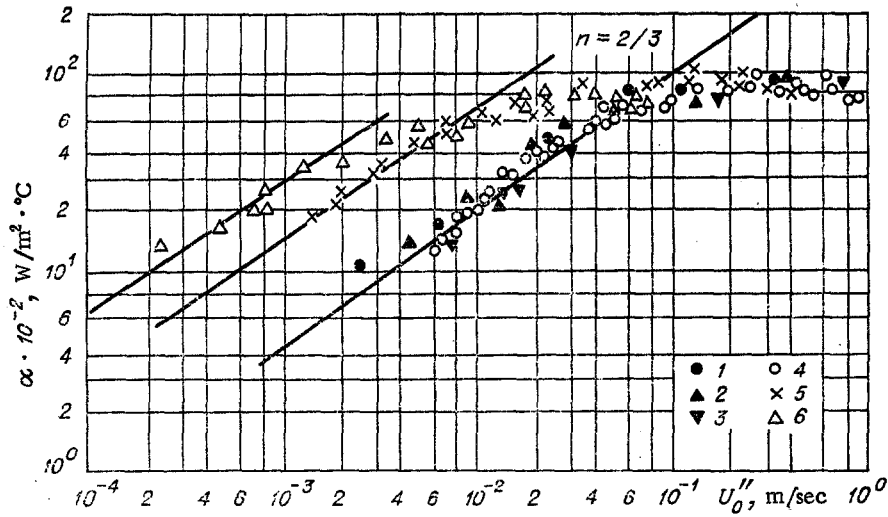
595

Fig. 2

$$R_{\min} = \frac{2\sigma T''}{r\rho''\Delta T}, \tag{1}$$

where ΔT is the initial superheating.

Internal Similarity Numbers for Gas—Liquid Flows. If the internal linear scales are introduced into the classical similarity numbers, one gets similarity numbers that are independent of the external geometrical characteristics of the flow. An important point is that this operation is not trivial and leads to essentially new dimensionless parameters.

For example, the Nusselt number can be written in the following form for a viscous-gravitational flow in a liquid film $\rho' \gg \rho''$:

$$Nu^* = \frac{\alpha}{\lambda'} \left(\frac{\nu'^2}{g} \right)^{1/3}, \tag{2}$$

while the Reynolds' number is as follows as constructed from the mean flow speed and the mean film thickness:

$$Re_{fi} = G'/\mu'.$$

Figure 1 employs these coordinates to represent the experimental data on heat transfer in the film condensation of the vapors of nonmetallic liquids (a for a vertical tube, b for a vertical series of horizontal tubes; experiments with water and freon vapors). The relationship describes the entire range of states of flow in the condensate film: laminar with a smooth external boundary, laminar with waves, and developed turbulence. The effects from cooling surface geometry and other parameters are small, i.e., the $Nu^*(Re_{fi})$ function reflects the main law of film condensation for nonmetallic vapors.

We introduce the linear scale for the capillary-gravitational interaction into the standard Archimedes number to get

$$Ar_* = \frac{\rho'^{1/2}\sigma^{3/2}}{\mu'^2 \left[g\left(1 - \frac{\rho''}{\rho'}\right) \right]^{1/2}}, \tag{3}$$

which characterizes the interaction of capillary, viscous, and gravitational forces within a gas—liquid mixture. In particular, this influences the occurrence and development of gravitational-capillary waves in a viscous liquid.

The number of (3) may be also treated as a measure of relationship between the freely arising formations of order δ_σ and the scale of the local viscous effect, as estimated from the scale of the propagation speed for gravitational-capillary perturbations u_σ:

$$Ar_*^{1/2} = \frac{\delta_\sigma u_\sigma}{\nu'}.$$

The latter expression can also be considered as some local Reynolds' number for capillary-gravitational-viscous interaction.
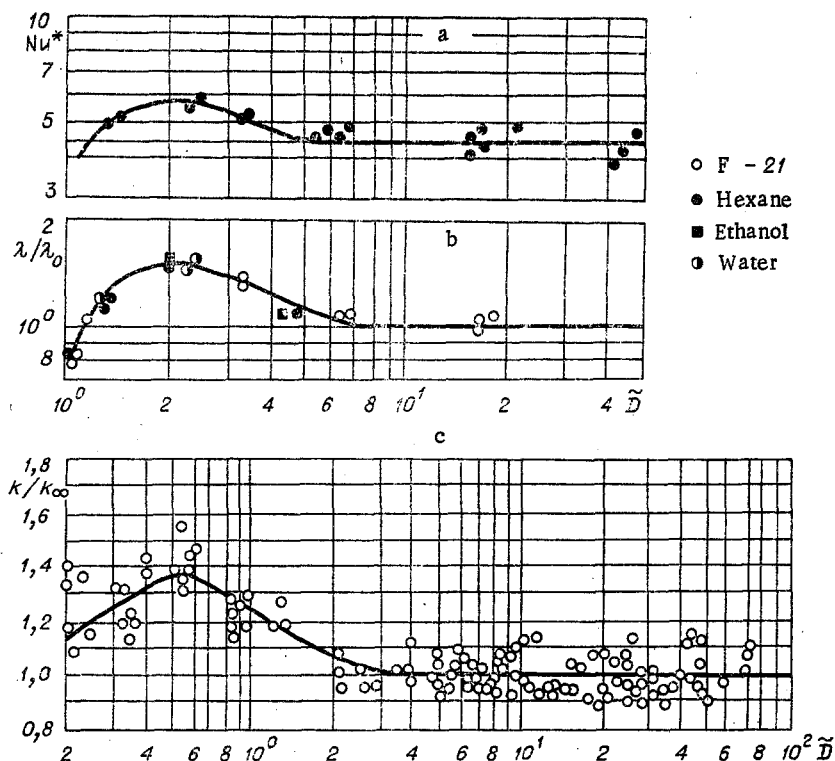
Fig. 3

To characterize the heat transfer from a surface passing bubbles or boiling, one can construct Nusselt and Peclet numbers of the form

$$\mathrm{Nu}_* = \frac{\alpha}{\lambda'}\left[\frac{\sigma}{g\,(\rho'-\rho'')}\right]^{1/2}, \quad \mathrm{Pe}_* = \frac{c'j''_{\mathrm{W}}}{\lambda'}\left[\frac{\sigma}{g\,(\rho'-\rho'')}\right]^{1/2}.$$

These numbers characterize the molecular and convective forms of heat transport in the liquid phase in response to the dynamic effects of the gas (vapor) generated at the surface.

A criterion for gasdynamic stability of a gas—liquid structure at a wall with free convection can be produced from the ratio of the dynamic pressure due to the gas (vapor) phase generated at the wall and the scale of the Archimedean force:

$$k = \frac{U''_{\mathrm{cr}}\,\rho''^{1/2}}{[\sigma g\,(\rho'-\rho'')]^{1/4}}. \tag{4}$$

An essentially new similarity number is the ratio of the scale for the propagation speed of capillary-gravitational waves to the isothermal velocity of sound in the gas phase:

$$\mathrm{M}_* = \left(\frac{\rho''}{p}\right)^{1/2}\left(\frac{g\sigma}{\rho'-\rho''}\right)^{1/4}.$$

This novel analog of the Mach number has a considerable effect on certain processes in gas—liquid flows at very low speeds.

Figure 2 shows the experimental data on the heat-transfer coefficient under conditions of free convection from a microporous plate to water in the presence of passing gas: 1) hydrogen, 1 atm; 2) helium, 1 atm; 3) argon, 1 atm; 4-6) nitrogen, 1, 6, and 16 atm, respectively. There is clearly a region of developed bubble passage in which approximately

$$\alpha \sim U''^{2/3},$$

and the absolute level is very much dependent on the pressure in the vessel (i.e., on the gas density under otherwise equal conditions), but it is largely insensitive to the type of gas (i.e., here the molecular weight).

In that case, changes in gas density due to variations in pressure and molecular weight are not equivalent, on account of the effects of M_*.
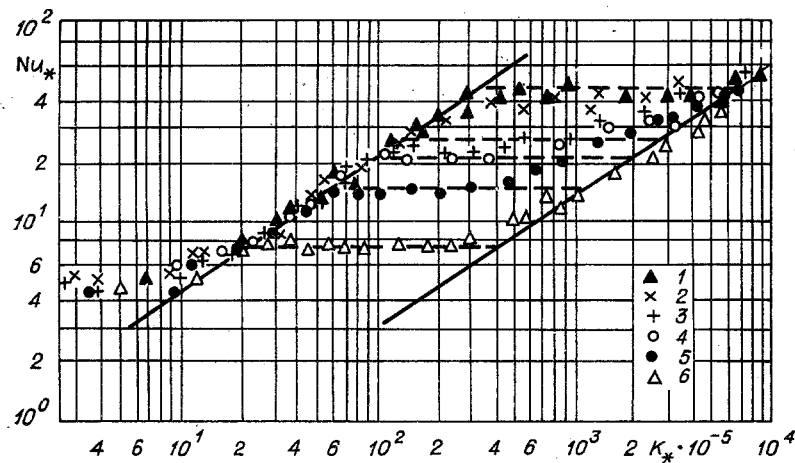
597

Fig. 4

The effects of system geometry on processes decisively governed by local phase interactions may be characterized as the ratio of the internal linear scales to the external ones. For example, self-modeling with respect to external geometrical parameters involves the fundamental relation between the internal similarity numbers in the gas—liquid mixture if

$$D \gg \delta_\sigma.$$

Figure 3 shows the effects of this factor on the heat transfer in laminar film condensation on a horizontal tube (a), on the criterion for transition from bubble boiling to film boiling in a large volume of saturated liquid (b), and on the wavelength at the surface of a freely flowing liquid film (c). In all cases, the maximum effect occurs for $\tilde{D} = D/\delta_\sigma$ and is clearly related to change in the length of the capillary-gravitational waves.

Self-Modeling in Liquid-Phase Viscosity. The turbulizing effect of discrete elements of one phase on the other means that there are extensive regions of Reynolds' numbers in which the integral characteristics of the energy and mass transfer in a gas—liquid mixture are independent of the viscosity. This is observed in liquid spraying by pneumatic means, in the motion of gas bubbles in circular pipes, and especially when the wall layer in a pipe is injected with gas or vapor. In the latter cases, the perturbing action of the generated light phase makes itself felt directly in the viscous sublayer at the wall, where molecular friction and thermal conduction occur. However, the molecular thermal conduction is then eliminated completely, since there is always the thermal resistance of a virtually immobile thin layer directly at the heating surface. In such a case, all the dynamic similarity numbers containing the viscosity are eliminated, together with the Prandtl number, which characterizes the diffusion relation for momentum and heat. This means that heat transfer in such a process is described by the same laws for metallic and nonmetallic liquids. The data of Fig. 4 on heat transfer from a porous surface to water and water—glycerol solutions injected with nitrogen and helium show that there is a basic relationship (left curve) for $Nu_*(K_*)$ that is self-modeling with respect to Ar_*, and also that there are regions that are virtually self-modeling with respect to the dynamic parameters, in addition to the right closing branch, which is again almost self-modeling with respect to the viscosity. In Fig. 4, the various values of Ar_* correspond to the following curves: 1) $1.26 \cdot 10^3$, 2) $1.21 \cdot 10^3$, 3) $0.865 \cdot 10^3$, 4) $0.621 \cdot 10^3$, 5) $0.296 \cdot 10^3$, 6) $0.046 \cdot 10^3$.

Figure 5 shows $\langle Nu_* \rangle$ in relation to Ar_* found on averaging the data for bubble injection into water and water—glycerol mixtures for a region approximately self-modeling for K_*. A notable point is that Nu_* in the form of (2) is constant to a first approximation, as in the approximately self-modeling region for film condensation of pure vapor.

Figure 6 shows the stability criterion of (4) in relation to the similarity number of (3) for the displacement of the water—glycerol mixture (1, helium; 2, nitrogen), and the same for water (3, hydrogen; 4, nitrogen; 5, helium), and the same for ethanol (6, argon; 7, nitrogen), in each case for a microporous bubble-injection surface with free convection. There is self-modeling with respect to the viscosity for Ar_* larger than a critical value.

Effects of Capillary-Acoustic Interaction. The data of Fig. 4 on heat transfer in developed bubble injection are described satisfactorily as follows for the first self-modeling region for the viscosity:
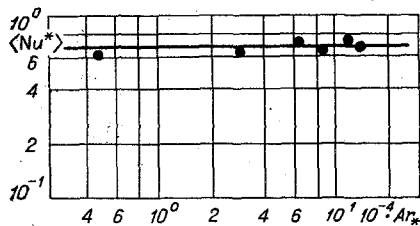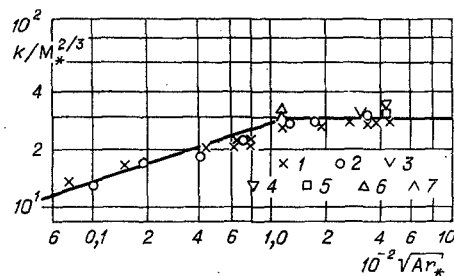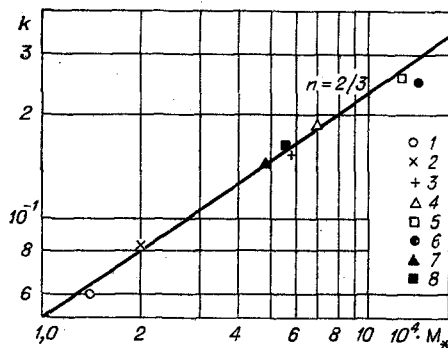
Fig. 5

Fig. 6

Fig. 7

$$\mathrm{Nu}_* \sim \left(\frac{\mathrm{Pe}_*}{\mathrm{M}_*^2}\right)^{2/3}, \tag{5}$$

where the following is the definitive similarity criterion:

$$K_* = \frac{c'U''p}{g\lambda'}, \tag{6}$$

in which only the thermal parameters (c' and λ'), the kinematic ones (U''), and the acoustic one (p) are retained. The effects of the surface tension appear in (5) only via Nu_*.

Figure 7 shows the stability criterion of (4) in relation to M_* for liquid displacement from a microporous surface by an injected bubbling gas in the region self-modeling with respect to Ar_* [water: 1) hydrogen, 2) helium, 3) nitrogen, 4) argon, 5) xenon, 6) SF_6; ethanol: 7) nitrogen, 8) argon]. The capillary-acoustic interactions have a very marked effect on the stability of the gas—liquid wall layer.

Phase-Transition Effects. Here we have the important fact that a phase transition may affect the self-modeling regions and (to some extent) the effects of the capillary-acoustic interactions on the stability of the gas—liquid wall layer.

Figure 8 shows data on heat transfer in developed bubble boiling as the ratio of the similarity number of (5) to Ar_* (1, water; 2, ethanol; 3, potassium; 4, sodium; 5, cesium; 6, Freon-21; 7, Freon-12; 8, nitrogen; 9, helium; 10, benzene). The evaporation has not altered the law of (5), which is characteristic of the first self-modeling region, but it has eliminated the effects of the viscosity in the working range of (6).

Figure 9 shows k in relation to M_* from data for the first crisis (transition from bubble boiling to film boiling) in a large volume of saturated liquid with free convection [1, water (p = 1.0-190 atm); 2, helium (0.6-2.07 atm); 3, propane (21.5-34.6 atm); 4, ethanol (0.06-42.2 atm); 5, hydrogen (0.92-12.1 atm); 6, methanol (1.0-63.5 atm); 7, benzene (0.16-47.0 atm); 8, oxygen (0.225-40.8 atm); 9, nitrogen (0.413-29.8 atm); 10, heptane (1.0-22.1 atm); 11, pentane (2.0-31.5 atm)]. The stability criterion remains virtually constant within the spread of the experimental points for a wide range in M_*. In the second boiling crisis, i.e., in the transition from film boiling to bubble boiling (e.g., as the temperature falls in a metallic component quenched in a liquid), the fundamental similarity numbers are as in the first crisis. However, the numerical value of the stability criterion k is much less.
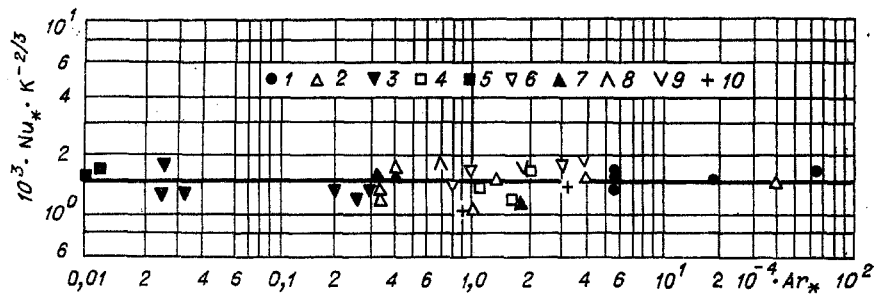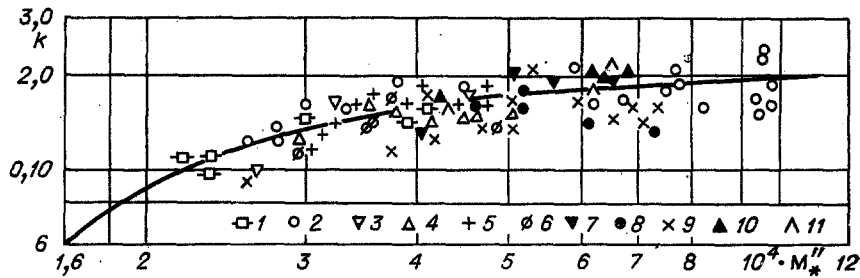
Fig. 8

Fig. 9

A phase transition also has a substantial effect on the stability criterion for change in the generation of gas and vapor bubbles at low pressures (below atmospheric), as is evident from the data in Fig. 10 (bubbling in water: 1, nitrogen; 2, helium; 3, water boiling).

<u>Convection of a Metastable Liquid.</u> Stable boiling at a heating surface requires the presence of numerous microscopic depressions due to the manufacturing technology that have dimensions greater than the critical nucleation radius defined by (1). In other words, the initial superheating of the wall layer of liquid above the equilibrium thermodynamic temperature for saturation on the plane should be

$$\Delta T_{min} \approx \frac{2\sigma T''}{r\rho''\delta_{i,m}},$$

where $\delta_{i,m}$ is the characteristic largest dimension of the active depressions.

Clearly, the vapor density is the basic physical parameter influencing superheating for a given substance. Therefore, effects due to nonboiling metastable wall layers are usually observed at pressures below atmospheric. The superheating in the wall layer, or in restricted volumes of liquid, may attain 100°K or more if the surface is very much depleted of virtual generation centers. Single-phase convection persists in such a metastable liquid, but when a certain critical superheating $\Delta T_{cr,3}$ is reached, this gives way explosively to film boiling. This we may call the third boiling crisis in large volumes.

An intermediate stage is generation of a cloud of microscopic bubbles in the wall region, which is initiated by the production of a few bubbles of radius R_{min} at the wall. One can characterize this process from the ratio of the work needed to produce the primary bubble to the momentum provided by it to the wall of metastable liquid:

$$\frac{\sigma R_{min}^2}{\rho' U_*^2 V_*}.$$

The best agreement with experiment is obtained if we assume $V_* \sim \delta_*$ and the characteristic velocity U_* is determined from the rate of growth of the vapor bubble at the solid wall:

$$\frac{dR}{dt} \sim \frac{\lambda' c' \rho'}{R}\left(\frac{\Delta T}{r\rho''}\right)^2.$$

This model is confirmed by experiments with ethanol, benzene, cesium, and potassium.

This study is based on many years of research on heat transfer in the condensation of vapors and boiling of liquids conducted by myself jointly with B. P. Avksentyuk, G. I. Bobrovich, I. I. Gogonin, I. G. Malenkov, et al., and it systematizes results in terms of
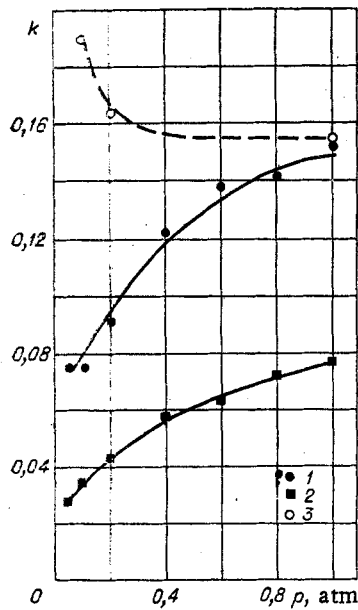
Fig. 10

the internal scales in gas—liquid systems. This approach to the thermohydrodynamics of poly-phase systems is particularly valuable, since many of these integral effects are only slightly dependent on the external parameters. For example, the heat-transfer rate is almost independent of the heater diameter and the liquid flow speed in developed bubble boiling. The initial data are derived from [1-4].

LITERATURE CITED

1. S. S. Kutateladze and I. G. Malenkov, "Gas-hydrodynamic aspects of heat transfer in liquid boiling," Teplofiz. Vys. Temp., No. 14(4) (1976).
2. B. P. Avksentyuk and S. S. Kutateladze, "Instability in heat transfer at surface depleted of vapor-formation centers," Teplofiz. Vys. Temp., 15, No. 1 (1977).
3. S. S. Kutateladze, "Heat transfer in boiling and bubbling in free convection in a liquid," Int. J. Heat Mass Transfer, 22, 281 (1979).
4. S. S. Kutateladze and I. I. Gogonin, "Heat transfer in film condensation of a slowly moving vapor," Int. J. Heat Mass Transfer, 22, 1593 (1979).